

Confinement-Induced Heat-Transport Enhancement in Turbulent Thermal Convection

Shi-Di Huang (黄仕迪), Matthias Kaczorowski, Rui Ni (倪睿), and Ke-Qing Xia (夏克青)

Department of Physics, The Chinese University of Hong Kong, Shatin, Hong Kong, China

(Received 10 July 2013; published 4 September 2013)

We report an experimental and numerical study of the effect of spatial confinement in turbulent thermal convection. It is found that when the width of the convection cell is narrowed, the heat-transfer efficiency increases significantly despite the fact that the overall flow is slowed down by the increased drag force from the sidewalls. Detailed experimental and numerical studies show that this enhancement is brought about by the changes in the dynamics and morphology of the thermal plumes in the boundary layers and in the large-scale flow structures in the bulk. It is found that the confined geometry produces more coherent and energetic hot and cold plume clusters that go up and down in random locations, resulting in more uniform and thinner thermal boundary layers. The study demonstrates how changes in turbulent bulk flow can influence the boundary layer dynamics and shows that the prevalent mode of heat transfer existing in larger aspect ratio convection cells, in which hot and cold thermal plumes are carried by the large-scale circulation along opposite sides of the sidewall, is not the most efficient way for heat transport.

DOI: [10.1103/PhysRevLett.111.104501](https://doi.org/10.1103/PhysRevLett.111.104501)

PACS numbers: 47.27.T-, 44.20.+b, 44.25.+f

The ability to significantly enhance the efficiency of heat transfer is of great importance in industry and in many daily applications. For example, efficient passive heat management is critical for many microelectronic devices. Here, using a classical model for convection, we show that a simple geometrical confinement can greatly increase the turbulent convective heat-transfer efficiency. Turbulent Rayleigh-Bénard (RB) convection, a fluid layer heated from below and cooled from above, is a paradigm for the study of general convection phenomena that occur ubiquitously in nature [1,2]. The system is characterized by three control parameters, i.e., the Rayleigh number Ra ($= \alpha g \Delta T H^3 / \nu \kappa$), the Prandtl number Pr ($= \nu / \kappa$), and the aspect ratio Γ (lateral dimension of the system over its height), where ΔT is the temperature difference across the fluid layer of height H , g the gravitational acceleration, and α , ν , and κ are the thermal expansion coefficient, kinematic viscosity, and thermal diffusivity of the convecting fluid, respectively. A major issue in the study of RB convection is how the nondimensional heat flux, the Nusselt number Nu (the ratio of actual flux over what would be transported by conduction alone), depends on the three control parameters. While Ra is a measure of the thermal driving strength and Pr measures the relative strengths of viscous and thermal diffusions of the system, the aspect ratio Γ characterizes the geometry and confinement effects of the convection cell and affects the structure and dynamics of the convective flow [3–12]. A dominant flow structure in RB convection is the so-called large-scale circulation (LSC). While different flow patterns are indeed observed in convection cells of different Γ [8,9], high-precision Nu measurements have shown that it has a weak dependence on Γ in both cylindrical and rectangular cells [4–6,12]. As Γ has a strong influence on the flow structures, this also suggests an insensitivity of heat

transport to the LSC [1]. Direct evidences for this insensitivity are provided by some novel experiments [13,14], where the LSC is dramatically perturbed but Nu changes little. These findings have led one to conclude that the LSC can hardly influence the overall heat transport in the system. Rather, the latter is primarily determined by the thermal boundary layers (BL). Indeed, so far, the only way to significantly change heat transport is to directly perturb the BL, such as by creating roughness on the conducting plates [15,16]. In this Letter, we present experimental and numerical studies of turbulent RB convection in quasi-2D geometries with varying aspect ratios. As Γ decreases, the system becomes more 2D-like and one would expect that the increased frictional drag from the sidewalls should decrease the heat transfer. On the contrary, our study reveals a significant enhancement of heat transport induced by the lateral confinement of the turbulent flows.

Five convection cells of rectangular shape are used in the experiment [17,18]. They have fixed height H and length L both being 12.6 cm, with varying width W equal to 7.56, 3.84, 2.56, 1.92, and 1.27 cm, respectively. The aspect ratio Γ_{\parallel} ($= L/H$) in the plane parallel to the LSC's circulation plane is thus one, whereas the aspect ratios in the planes perpendicular to the LSC, Γ_{\perp} ($= W/H$, hereafter simply Γ), have values 0.6, 0.3, 0.2, 0.15, and 0.1, respectively. The dimensions H , L , and W correspond to z , x , and y in the Cartesian coordinates and the same coordinates are used in the numerical setup. The Nu measurements were made in the range $8.6 \times 10^7 \leq Ra \leq 2.5 \times 10^9$, with the mean temperature T_c of the bulk fluid maintained at 40.0°C ($Pr = 4.3$). To reduce the influence of surrounding temperature fluctuations and minimize heat leakage, the convection cell is wrapped with several layers of thermal insulation and is placed in a thermostat (temperature variation $\leq 0.1^\circ\text{C}$).

Direct numerical simulations (DNS) of the Boussinesq equations were made using a finite volume solver for nonequidistant meshes in all coordinate directions and staggered grids for the three velocity components [19]. The Cartesian geometries are discretized such that the grid spacing is the same in the horizontal and the vertical directions of the square x - z plane, so that the boundary layers of the horizontal and vertical walls are equally well resolved and exceeding the requirements proposed in [20] for resolving the boundary layers. The grid spacing in the center of the geometry is equidistant and smaller than the global estimates of the Kolmogorov scale and comparable to the Batchelor scale. The grid spacing in the y direction is chosen such that at the wall and in the bulk it is comparable to those in the other two directions. We made an *a posteriori* analysis of the local resolution profiles through the center of the cells, showing that all relevant turbulent scales are sufficiently resolved. Furthermore, the global Nu computed from volume integrations of the thermal and kinetic dissipation rates are found to be virtually identical with Nu computed from averages over horizontal slices. The conditional averaging used to characterize the properties of the plumes in the flow is based on the idea that a hot (cold) plume must be hotter (colder) than its surrounding fluid in order to rise upwardly (go down). Therefore, we define a thermal plume as a region of a horizontal slice for which $\pm[T(x, y) - \langle T \rangle_{xy}] > c\langle T_{rms} \rangle_{xy}$ (where + is for a hot plume and - for a cold plume), leaving the remainder of the slice as the bulk flow. We furthermore require this region to carry an excess of heat in the vertical direction, i.e., $j_z(x, y) > cNu_{\text{global}}$, where $j_z = (RaPr)^{1/2}wT$ is the vertical convective heat flux expressed in the nondimensional variables used in the code [19], c is an empirical parameter chosen to be 0.8, and the subscript xy denotes averaging over the respective horizontal slice.

In Fig. 1, we show a semi-log plot of the experimentally measured normalized Nu versus Γ for several values of Ra. We find that the measured Nu for $\Gamma = 0.6$ are the same as those measured in a cylindrical cell of $\Gamma = 1$ in their overlapping range of Ra [21], which suggests that the effect of confinement is negligible at $\Gamma = 0.6$. It is known that the LSC is a quasi-2D structure with a width of about a half cell lateral dimension [22], so that the drag from the front and back walls does not affect the LSC a lot at this Γ . As Γ decreases from 0.6 to 0.3, however, Nu shows a decrease, which may be attributed to the increased drag due to the confinement. However, when the degree of confinement is further increased as Γ decreases from 0.3 to 0.2, rather than continue to decrease, Nu becomes larger than that in the larger Γ cells. This trend continues to the smallest Γ explored in the experiment. For $\Gamma = 0.1$, we find Nu is increased by $\sim 17\%$ for $Ra = 8.6 \times 10^7$ and $\sim 11\%$ for $Ra = 2.5 \times 10^9$. This is rather surprising and also counterintuitive, because in a highly confined space the drag force from the walls should slow down the fluid

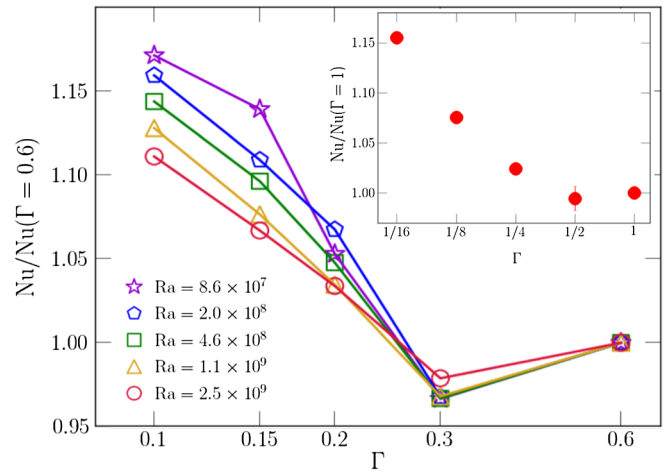


FIG. 1 (color online). Experimentally measured normalized global Nu vs Γ for five values of Ra. The solid lines are drawn to guide the eye. The error bars are all smaller than the symbol size. Inset: Normalized global Nu vs Γ obtained from DNS conducted at $Pr = 4.3$ and $Ra = 1 \times 10^9$.

motion and, therefore, inhibit the vertical heat transport. We note that for the combination of the working fluid (water) and the Plexiglas sidewall (4 mm thick), the thermal coupling between the fluid and sidewalls is negligible [1] and thus cannot account for this remarkable enhancement. From power-law fits to the measured Nu vs Ra for each Γ , we obtain scaling exponents in the range from 0.27 to 0.29. These values are in general agreement with those found in previous studies in the same parameter range and indicate that the turbulent flow is still in the so called “classical” regime of thermal convection [1], i.e., the heat transport should still be controlled mainly by the thermal BLs.

Using a small thermistor placed at cell center, we find that with decreasing Γ the local temperature fluctuation increases significantly and its probability density function (PDF) changes from exponential to Gaussian-like. A Gaussian-like PDF in the cell center can arise when more plumes are passing through that region and an exponential-like PDF has been attributed to the lack of plumes [14]. This suggests that the spatial distribution of thermal plumes has changed as a result of the confinement. It is well-known that the LSC is essentially an organized motion of plumes [23]. Thus, changes in the spatial distribution of plumes should be reflected in the flow pattern. Indeed, particle image velocimetry measurements at $Ra = 1.1 \times 10^9$ reveal that the single-roll LSC, while it still exists in $\Gamma = 0.3$, has disappeared in the $\Gamma = 0.15$ cell and its maximum mean velocity is reduced by 22% compared to the $\Gamma = 0.3$ case [21]. Thus, the fact that the global Nu shows an overall increase despite the decreased flow velocity suggests that something has happened that is able to offset the effect of drag.

To gain insight into how heat transfer is increased by confinement, we perform DNS studies in several cells with

$\Gamma = 1, 1/2, 1/4, 1/8,$ and $1/16$ at fixed $Pr = 4.3$ and $Ra = 1 \times 10^9$. The $\Gamma = 1$ cell is a cube and the smaller Γ cells are rectangular ones similar to those used in the experiment. The inset of Fig. 1 shows a semi-log plot of normalized Nu vs Γ . It is seen that Nu first decreases when Γ changes from 1 to $1/2$ and then becomes larger than the $\Gamma = 1$ value when $\Gamma \leq 1/4$, achieving enhancement $\approx 16\%$ when $\Gamma = 1/16$. This is similar to the experimental finding that Nu first decreases when Γ changed from 0.6 to 0.3 and then increases afterwards. If we interpolate the numerical results to $\Gamma = 0.1$, we find a Nu enhancement of about 10%, which is in good agreement with the experimental result of $\sim 12\%$ for the same values of Γ and Ra . Thus, the DNS result confirms the experimental finding. As the cubic cell has a complicated flow pattern with the LSC lying in a diagonal plane [22], we use it only as a reference for the global Nu and will hereafter focus on the rectangular cells.

Figure 2 shows horizontal slices of instantaneous temperature and velocity fields at a distance $z \approx 2\delta_{th}$ above the bottom plate (δ_{th} is the thermal BL thickness). In the figure, the red and blue structures correspond to hot and cold plumes. It is seen that, for the $\Gamma = 1/2$ cell, cold plumes are brought down by the LSC mostly along one side of the cell so that they predominantly fall on one region of the plate [the left side in Fig. 2(a)], and the spreading fluid generated by the impingement pushes the hot plumes away and mostly in one direction (to the right). As the hot plumes propagate, they merge and convolute to form spiraling structures. Moreover, these hot plumes generally rise from the other side of the plate, i.e., they typically traverse the length of the plate. This is exactly what has been observed experimentally in a cylindrical cell [24]. In fact, this is the paradigmatic mode of heat transfer

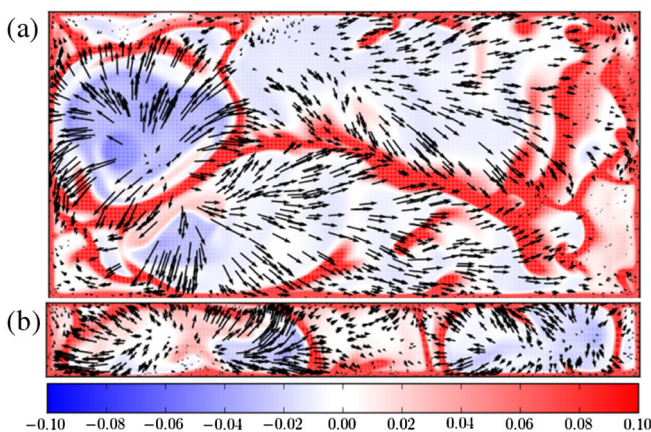


FIG. 2 (color online). Instantaneous temperature and velocity fields (from DNS) in a horizontal plane at a distance $z \approx 2\delta_{th}$ above the bottom plates: (a) $\Gamma = 1/2$ and (b) $\Gamma = 1/8$. The temperature is coded in color in the unit of ΔT such that it is zero at cell center, and the velocity is coded in vector length in units of free-fall velocity.

in turbulent RB convection when a LSC exists, i.e., the single-roll LSC carries cold plumes falling down on one side of the plate and hot plumes going up from the other side; as a result, the “heat-carrying” plumes only occasionally go through the cell center [25]. The situation is changed in the $\Gamma = 1/8$ cell. As a stable single-roll LSC no longer exists, the cold plumes are brought down by the flow at random positions in the bottom plate [Fig. 2(b)]. At the same time, the lateral confinement also changes the plume morphology in the BL, i.e., the plumes now extend the entire lateral (y) width of the plate. As a result of this confinement, the plume’s motion in the plate becomes one dimensional. It is seen that as the hot plumes are pushed toward each other by the splashing cold plumes, they have nowhere to go but collide with each other head-on, merge, and then go up (see also the movies in the Supplemental Material [26]). This can be seen directly from the vertical slices of the instantaneous temperature and velocity fields shown in the top panel of Fig. 3. It is also seen that in smaller Γ geometries the plumes are more coherent and energetic, i.e., the hot and cold plumes are respectively hotter and colder and, thus, carry more “heat.” For the $\Gamma = 1/4$ cell, the situation is somewhere in between the $1/2$ and the $1/8$ cells, and the $1/16$ geometry is qualitatively the same as in the $1/8$ case. In the bottom panel of Fig. 3, we

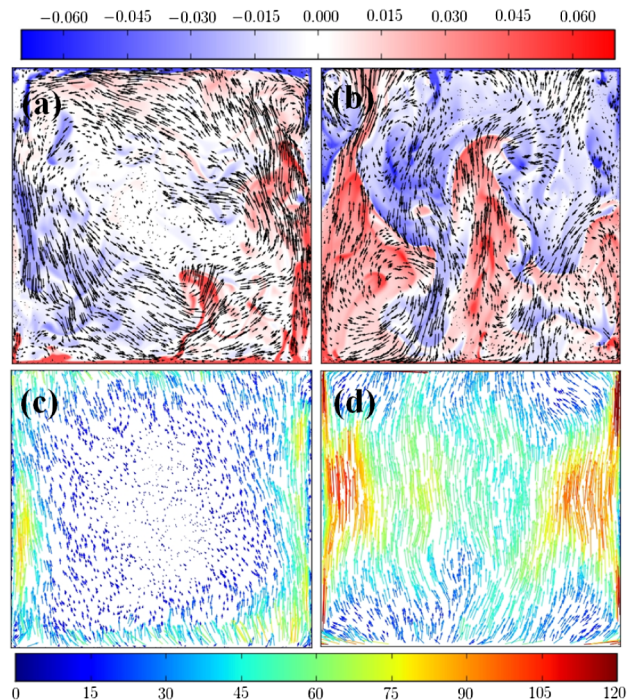


FIG. 3 (color online). Instantaneous temperature-velocity fields (top panel) and time-averaged local heat flux (bottom panel) in the vertical x - z plane midway between the lateral y walls (from DNS) for $\Gamma = 1/2$ (left) and $\Gamma = 1/8$ (right). The temperature and velocity codings are the same as in Fig. 2. The nondimensional heat flux is coded in both color scale and vector length.

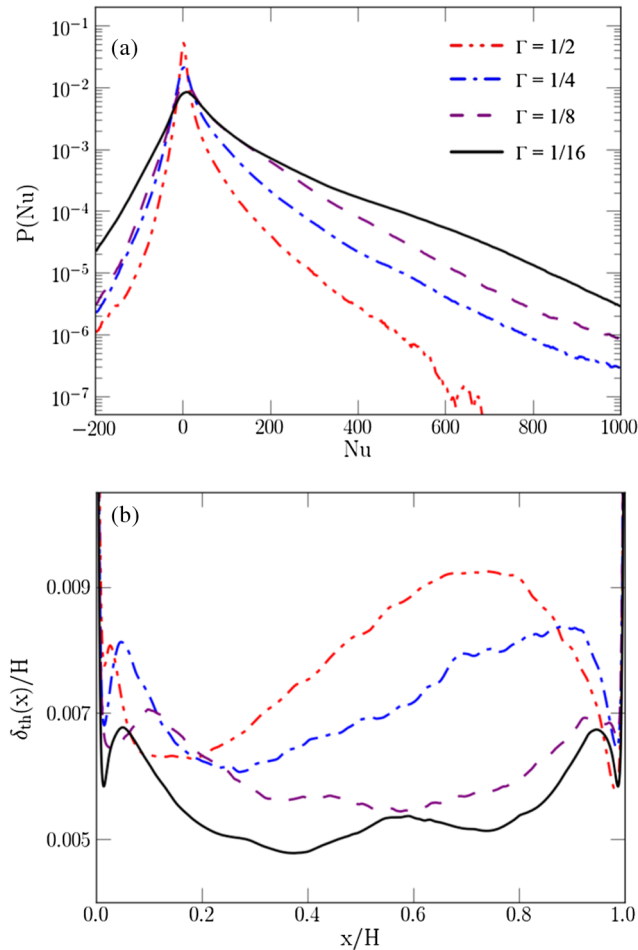


FIG. 4 (color online). (a) PDFs of the local Nu averaged over the volume $3/8 \leq x/L, y/W, z/H \leq 5/8$ in the center of the cell for different Γ . (b) The thermal boundary layer thickness $\delta_{th}(x)$ along the bottom plate (determined from temperature profiles using the “slope” method [9]).

show the time-averaged local $Nu(x, z)$ obtained in the central vertical plane ($y = 0$), which illustrates how the spatial confinement has not only increased the global Nu , but also changed the way heat is transported in the cell, i.e., heat transport is no longer confined in the periphery region but takes place in the entire cell. This fact is also evident in the PDF of the local Nu measured in the bulk region of the cell. As shown in Fig. 4(a), very large values of the instantaneous Nu occur with much higher probabilities in the smaller Γ cells, suggesting the existence of more energetic events in the highly confined geometries. Using the plume extracting algorithm, we find that the average temperature of a hot plume in $\Gamma = 1/16$ is 16% higher than that in $\Gamma = 1/2$ at a height of $z/H = 0.2$, but becomes 30% higher at $z/H = 0.8$ (similarly for cold plumes), suggesting that plumes in smaller Γ cells lose their temperature contrast more slowly in spite of moving slower. As a consequence, the hot (cold) plumes are able to warm up (cool down) the top (bottom) plates more effectively,

making the thermal BL thinner. As shown in Fig. 4(b), with decreasing Γ , the BL thickness δ_{th} indeed becomes more uniform and on average thinner. We remark that the present quasi-2D system is very different from the true 2D case, which can exhibit complicated Nu - Γ relationships [27]. It is clear that in the quasi-2D cell, the front and back walls (that are absent in the 2D case) play important roles, i.e., they generate mixing in the bulk and also inhibit the LSC so plumes can now impinge all over the plates.

Based on the above analysis, we arrive at the following physical picture. First, the confinement leads to increased frictional drag from the walls, which in turn significantly weakens the LSC and eventually suppresses it for the highly confined cases. This enables thermal plumes to impinge over the entire boundary layers. When this is coupled with changes in the plume morphology in the boundary layer, they result in emissions of more coherent and energetic plumes that lead to the overall enhancement of the global Nu , despite the increased drag from the walls. These geometrical confinement-induced effects provide a new paradigm for how changes in the bulk can influence the boundary layer in turbulent flows. We expect the results from this study to find applications in many practical problems in passive heat management, such as the design of cooling devices in the microelectronics industry.

We thank F. Wang and K. L. Chong for their help with the experiment and simulation. We gratefully acknowledge the use of the computational resources of the Leibniz-Rechenzentrum Munich under Project No. pr63ro and the High Performance Cluster Computing Centre, Hong Kong Baptist University, which receives funding from the Hong Kong Research Grants Council (RGC), and support of this work by the RGC under Project No. CUHK403811.

- [1] G. Ahlers, S. Grossmann, and D. Lohse, *Rev. Mod. Phys.* **81**, 503 (2009).
- [2] D. Lohse and K.-Q. Xia, *Annu. Rev. Fluid Mech.* **42**, 335 (2010).
- [3] S. Grossmann and D. Lohse, *J. Fluid Mech.* **486**, 105 (2003).
- [4] D. Funfschilling, E. Brown, A. Nikolaenko, and G. Ahlers, *J. Fluid Mech.* **536**, 145 (2005).
- [5] A. Nikolaenko, E. Brown, D. Funfschilling, and G. Ahlers, *J. Fluid Mech.* **523**, 251 (2005).
- [6] C. Sun, L.-Y. Ren, H. Song, and K.-Q. Xia, *J. Fluid Mech.* **542**, 165 (2005).
- [7] J. Niemela and K. R. Sreenivasan, *J. Fluid Mech.* **557**, 411 (2006).
- [8] R. du Puits, C. Resagk, and A. Thess, *Phys. Rev. E* **75**, 016302 (2007).
- [9] C. Sun, Y.-H. Cheung, and K.-Q. Xia, *J. Fluid Mech.* **605**, 79 (2008).
- [10] J. Bailon-Cuba, M. S. Emran, and J. Schumacher, *J. Fluid Mech.* **655**, 152 (2010).
- [11] H. Song and P. Tong, *Europhys. Lett.* **90**, 44001 (2010).

- [12] Q. Zhou, B.-F. Liu, C.-M. Li, and B.-C. Zhong, *J. Fluid Mech.* **710**, 260 (2012).
- [13] S. Ciliberto, S. Cioni, and C. Laroche, *Phys. Rev. E* **54**, R5901 (1996).
- [14] K.-Q. Xia and S.-L. Lui, *Phys. Rev. Lett.* **79**, 5006 (1997).
- [15] Y. Shen, P. Tong, and K.-Q. Xia, *Phys. Rev. Lett.* **76**, 908 (1996).
- [16] Y.-B. Du and P. Tong, *Phys. Rev. Lett.* **81**, 987 (1998).
- [17] K.-Q. Xia, C. Sun, and S.-Q. Zhou, *Phys. Rev. E* **68**, 066303 (2003).
- [18] K. Sugiyama, R. Ni, R. J. A. M. Stevens, T. S. Chan, S.-Q. Zhou, H.-D. Xi, C. Sun, S. Grossmann, K.-Q. Xia, and D. Lohse, *Phys. Rev. Lett.* **105**, 034503 (2010).
- [19] M. Kaczorowski and K.-Q. Xia, *J. Fluid Mech.* **722**, 596 (2013).
- [20] O. Shishkina, R. J. A. M. Stevens, S. Grossmann, and D. Lohse, *New J. Phys.* **12**, 075022 (2010).
- [21] S.-D. Huang and K.-Q. Xia (to be published).
- [22] X.-L. Qiu and K.-Q. Xia, *Phys. Rev. E* **58**, 5816 (1998).
- [23] H.-D. Xi, S. Lam, and K.-Q. Xia, *J. Fluid Mech.* **503**, 47 (2004).
- [24] Q. Zhou, C. Sun, and K.-Q. Xia, *Phys. Rev. Lett.* **98**, 074501 (2007).
- [25] X.-D. Shang, X. L. Qiu, P. Tong, and K. Q. Xia, *Phys. Rev. Lett.* **90**, 074501 (2003).
- [26] See Supplemental Material at <http://link.aps.org/supplemental/10.1103/PhysRevLett.111.104501> for movies of the instantaneous temperature and velocity fields (from DNS) in both the horizontal plane (near bottom plate) and the vertical plane (midway between the front and back walls) for $\Gamma = 1/2$, $1/8$, and $1/16$, respectively.
- [27] E. P. van der Poel, R. J. A. M. Stevens, and D. Lohse, *Phys. Rev. E* **84**, 045303(R) (2011).